Asian Journal of Chemistry; Vol. 32, No. 6 (2020), 1297-1302

ASIAN JOURNAL OF CHEMISTRY

https://doi.org/10.14233/ajchem.2020.22516

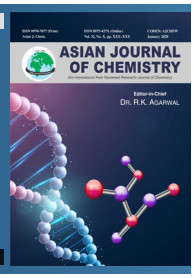

Binding of Methyl Viologen and its Radical to *p*-Sulfonatocalix[4]arene

MUKTAR SHAIKH* and JAYSHREE K. KHEDKAR

Department of Chemistry, Shri Anand College, Pathardi-414102, India

*Corresponding author: Tel./Fax: + 91 2428 222736; E-mail: shaikh.muktar@rediffmail.com

Received: 26 October 2019; *Accepted*: 26 December 2019; *Published online*: 30 May 2020; AJC-19873

Binding of *N*,*N*′-dimethyl-4,4′-bipyridinium (methyl viologen, MV^{2+}) and its radical ($MV^{+\bullet}$) to novel *p*-sulfonatocalix[*n*]arene (CX[4]-S,) host has been investigated using the density functional theory (DFT). The hydrogen bonded interactions between α-, β- and -CH_3 protons of methyl viologen with SO_3^- groups of CX[4]-S render stability to their complexes. In the lowest energy structures, one of the methyl groups of MV^{2+} was partially penetrated within the cavity of CX[4]-S host owing to C-H···O interactions with upper rim of host while the remaining methyl group excluded from the cavity. The radical $MV^{+\bullet}$ revealed qualitatively similar binding patterns to CX[4]-S host as that of MV^{2+}. Moreover, interaction energy of methyl viologen dication was predicted to be larger than that of the corresponding radical cation.

Keywords: Calixarene, Viologens, Density functional theory, Molecular electron density topography, Hydrogen bonding.

INTRODUCTION

The family of calixarene (CX[*n*]) hosts [1] has been of growing interest in catalysis [2], supramolecular chemistry [3,4] and biological sciences [5-7]. The bowl-shaped cavities with varying dimensions in which cations and neutral organic as well as inorganic guests can easily be encapsulated make these hosts fascinating [8,9]. The versatility of CX[*n*] framework has been explored to synthesize array of functionalized hosts by substitution on either or both rims which renders them with remarkable selectivity and bindings [9-12]. Seiji *et al*. [13] demonstrated the solubility of CX[*n*] macrocycles in aqueous solutions, which can be enhanced with suitable substitution of sulphonato groups at the upper rim. These modified hosts find applications in catalysis, separation techniques and sensors [14-16].

To understand inhibition of viologen toxicity, ^{1}H NMR and X-ray crystallography experiments [17] have been carried out on host-guest complexes of *p*-sulphonatocalix[4]arenes (CX[4]-S) and viologens. Pursuant to this in the present work, the binding patterns of CX[4]-S with *N*,*N*′-dimethyl-4,4′-bipyridinium (methyl viologen) as guests were analyzed. The viologen guest comprising of two pyridinium rings joined at *para*-positions [18] have ability to exist in three well characterized oxidation states *viz*. dication, radical cation and neutral forms, which is crucial in their use as redox indicators, electrochemical display devices [19], biological systems and herbicidal activity [20,21]. The ease of reduction and exceptionally long life-time with strong absorption in the visible spectral range make the $MV^{+\bullet}$ radical particularly interesting. Moreover, viologens can be transformed into corresponding radical cations and neutral molecules either chemically or electrochemically [22,23]. It should be remarked here that the stabilization of viologen radical cation ($MV^{+\bullet}$) *via* chemical modification is crucial in reversible π-dimerization [24]. Ong and Kaifer [25] reported that dimerization of viologen dications and radicals can be prevented by complexation with cucurbit[7]uril. Experimental investigations [26,27] on binding behaviour and thermodynamics of CX[4]-S and CX[5]-S with methyl viologen (MV^{2+}) and its radical form have demonstrated that selectivity and binding abilities of CX[4]-S and CX[5]-S hosts were dramatically pH-controlled. From the above discussion, it is clear that the complexation of CX[n]-S hosts have widely been studied experimentally. Nonetheless detailed theoretical studies on these complexes have not been reported yet. To this direction we utilized density functional theory to derive molecular level insights for interactions between CX[4]-S host and MV^{2+} and its corresponding $MV^{+\bullet}$ radical.

This is an open access journal, and articles are distributed under the terms of the Attribution 4.0 International (CC BY 4.0) License. This license lets others distribute, remix, tweak, and build upon your work, even commercially, as long as they credit the author for the original creation. You must give appropriate credit, provide a link to the license, and indicate if changes were made.

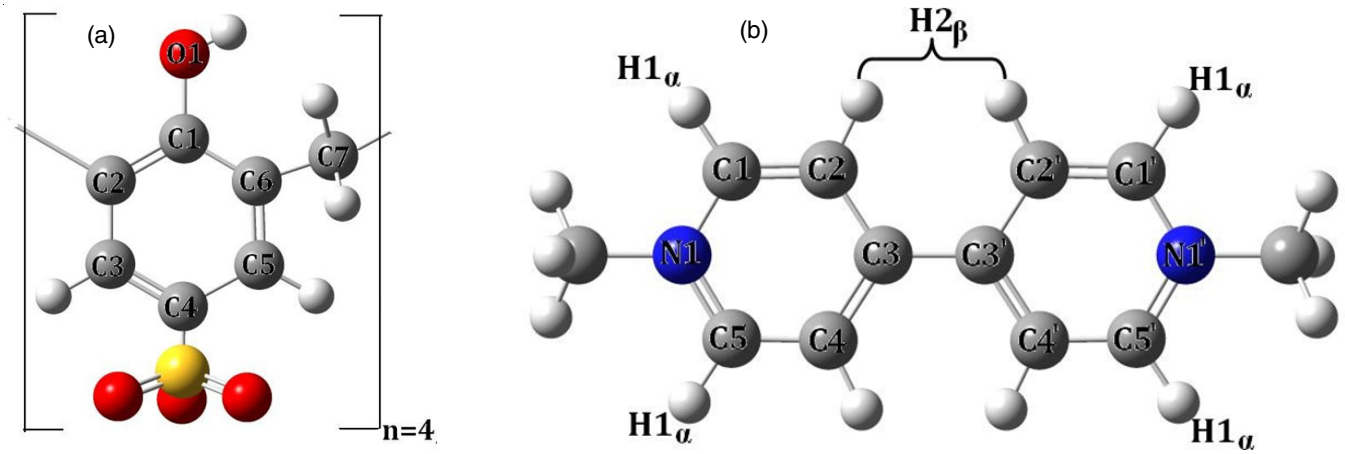

Fig. 1. Atomic numbering scheme in (a) CX[*n*] monomer and (b) methyl viologen

COMPUTATIONAL METHODS

Molecular electrostatic potential (MEP) of CX[4]-SO_3H hosts characterize the effective electron-rich regions, which are largely localized near SO_3H groups at the upper rim. Thus, the guidelines for electrophile binding can be derived. Accordingly different conformers of CX[4]-S-MV^{2+} and CX[4]-S-$MV^{+\bullet}$ were devised wherein the methyl group of guest directing toward the MEP critical points in CX[4]-S macrocycle. A detailed review of MEP and its topography can be found in the literature [28-31]. The complexes thus obtained were subjected to optimize by employing semi-empirical PM6 quantum chemical calculations. Subsequently, the structures exhibiting qualitatively different host-guest binding patterns with CX[4]-S hosts bound to MV^{2+} and its radical were optimized within the framework of density functional theory incorporating Becke′s three parameter exchange (B3) [32], coupled with Lee, Yang, and Parr′s (LYP) [33] correlational functional and stand alone M06 functional due to Truhlar and Zhao [34] using Gaussian 09 program [35]. The internally stored 6-31G(d,p) basis set was employed. Moreover, the calculations at the B3LYP/6-31++G(d,p) level of theory were performed for CX[4]-S host and its MV^{2+} complex. Interaction energies in these host-guest complexes were calculated by subtracting the sum of electronic energies of the host and viologen guest from that of its complex. An excellent review of MEP topography can also be found in the literature [36-39]. NMR chemical shifts (δ) were calculated by subtracting the nuclear magnetic shielding tensors of protons of host (or guests) from those in TMS (as a reference) using the gauge-independent atomic orbital (GIAO) method [40]. The effect of solvent (water) on the electronic structure and ^{1}H NMR chemical shifts were simulated *via* self-consistent reaction field (SCRF) calculations incorporating polarizable continuum model (PCM) [41].

RESULTS AND DISCUSSION

The atomic numbering scheme and optimized geometries of CX[*n*]-S monomer and methyl viologen are displayed in Fig. 1. The B3LYP optimized geometries of CX[4]-S revealed a cone conformer (Fig. 2) to be stable which has partly been attributed to extended hydrogen-bonding network. It was pointed that host-guest interactions of CX[4]-S were facilitated *via*

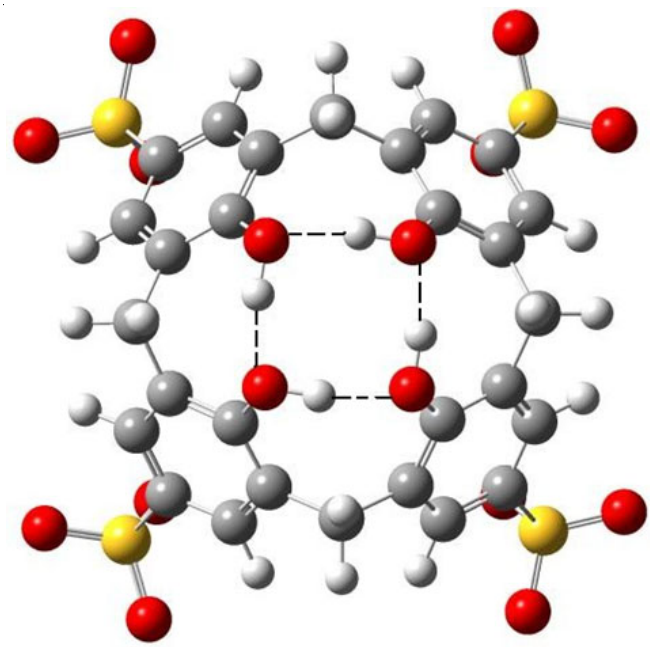

Fig. 2. Cone conformer in CX[4]-S host

SO_3^- substituents, electron-rich regions of macrocyclic hosts. The B3LYP optimizations in gas phase converged to only one conformer in each case. The MV^{2+} complexes of CX[4]-S are shown in Fig. 3. Geometrical parameters of isolated and MV^{2+} complexed CX[4]-S thus obtained are given in Table-1. A comparison of these data with those obtained from M06 functional is shown in Table-1. It may be noted that M06 functional accounts for non-covalent dispersion host-guest interactions. Moreover, the complex structure in gas phase obtained from B3LYP and M06 based calculations are rather similar. Use of M06 functional in the density functional theory yield CX[4]-S-MV^{2+} complex wherein two pyridinium rings of MV^{2+} guest attain (nearly) planar configuration (< C2′-C3-C3′-C4′ being 176º). The B3LYP calculations engender a complex with non-planar pyridine rings in the dication guest (Table-1). A comparison of structural parameters in the complex obtained from M06 and B3LYP based calculations revealed that except for the C6-C7 bond distance which differ by 0.014 Å, the remaining bond distances or bond angles do not vary significantly. The density functional calculations in gas phase further shows MV^{2+}

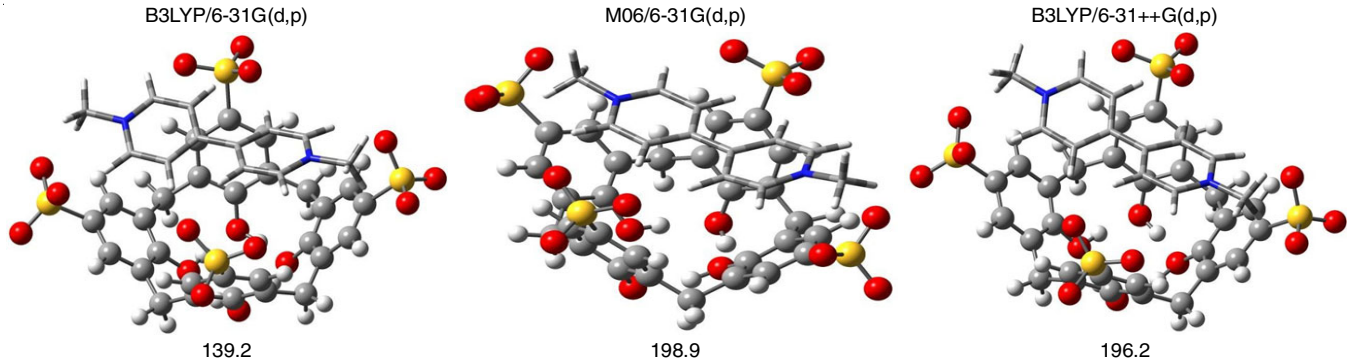

Fig. 3. Lowest energy CX[4]-S-MV^{2+} complexes optimized using B3LYP and M06 functional. Interaction energies (kJ mol^{-1}) given in parentheses

TABLE-1
A COMPARISON OF OPTIMIZED GEOMETRICAL PARAMETERS (BOND DISTANCES IN Å AND BOND ANGLES IN °) OF CX[4]-S, MV^{2+} AND CX[4]-S-MV^{2+} COMPLEX USING B3LYP AND M06 FUNCTIONALS

				CX[4]-S-MV^{2+}		
	6-31G(d,p)		6-31G++(d, p)	6-31G(d, p)		6-31G++(d, p)
CX[4]-S	B3LYP	M06	B3LYP	B3LYP	M06	B3LYP
O1–H1	1.000	0.988	0.986	0.991	0.981	0.990
O1–C1	1.385	1.377	1.384	1.384	1.373	1.386
C1–C2	1.407	1.402	1.407	1.406	1.400	1.407
C2–C7'	1.536	1.522	1.537	1.527	1.513	1.528
C2–C3	1.400	1.395	1.400	1.398	1.392	1.399
C3–C4	1.396	1.391	1.399	1.395	1.390	1.396
C4–C5	1.396	1.390	1.398	1.394	1.389	1.395
C5–C6	1.402	1.397	1.402	1.399	1.394	1.401
C6–C1	1.408	1.403	1.408	1.406	1.401	1.407
C6–C7	1.537	1.523	1.539	1.529	1.515	1.530
C2–C7–C6	119.2	118.2	116.6	115.0	116.3	115.0
C7–C6–C1	122.2	122.3	121.4	121.9	119.7	122.5
C6–C1–O1	120.1	120.3	120.2	121.0	120.4	120.8
O1–C1–C2	117.0	117.0	116.9	118.2	119.2	117.0
C1–C2–C7'	121.6	121.6	120.7	120.1	119.3	121.3
C1–C2–C3	117.3	117.5	117.7	118.8	119.6	118.0
C2–C3–C4	121.4	121.3	121.0	120.3	119.9	120.9
C3–C4–C5	119.3	119.4	119.8	120.1	120.5	119.9
C4–C5–C6	121.6	121.5	121.3	120.8	119.9	121.2
C5–C6–C1	117.1	117.2	117.4	118.7	118.7	117.6
MV^{2+}						
C1-$H1_{\alpha}$	1.084	1.086	1.084	1.086	1.086	1.087
C2-$H2_{\beta}$	1.084	1.086	1.084	1.089	1.091	1.087
C3-C3'	1.489	1.480	1.490	1.484	1.477	1.485
C6-N1	1.491	1.482	1.492	1.481	1.471	1.482
C2-C3-C3'-C4'	139.6	141.1	138.2	158.6	176.5	156.4

cation lies horizontally at upper rim of the host in its CX[4]-S complex facilitating C-H···O interactions with SO_3^- groups on the upper rim of host. The calculations at the B3LYP/6-31++G (d,p) level of theory revealed the identical structure for the CX[4]-S-MV^{2+} complex as that of B3LYP/6-31G(d,p). A comparison of optimized geometrical parameters is given in Table-1. On the other hand, experimental studies with ^1H NMR and isothermal titration calorimetry experiments [27] point to complex structure in which MV^{2+} was immersed into CX[4]-S cavity with penetration of methyl group. In order to account for this discrepancy both CX[4]-S complexes along with their individual host and guest gas phase structures were subjected to SCRF-PCM optimizations.

The SCRF-PCM optimized structures of CX[4]-S-MV^{2+} complex are displayed in Fig. 4. Contrary to gas phase structure the SCRF derived structure revealed one of the methyl groups partially penetrating within the cavity of CX[4]-S host owing to C-H···O interactions with upper rim of host while the remaining methyl group excluded from the cavity. Thus, the structure thus derived possesses five C-H···O interactions from methyl, α-, β-protons and host portal (Fig. 4). Bader [38] showed that the strength of hydrogen bonding interactions can be correlated to the electron density at the bcp (ρ_{bcp}) in MED topography. The ρ_{bcp} values for complexes of MV^{2+} with CX[4]-S hosts are given in Table-2. It may thus be conjectured that stability of the complex was governed by the number and strength of

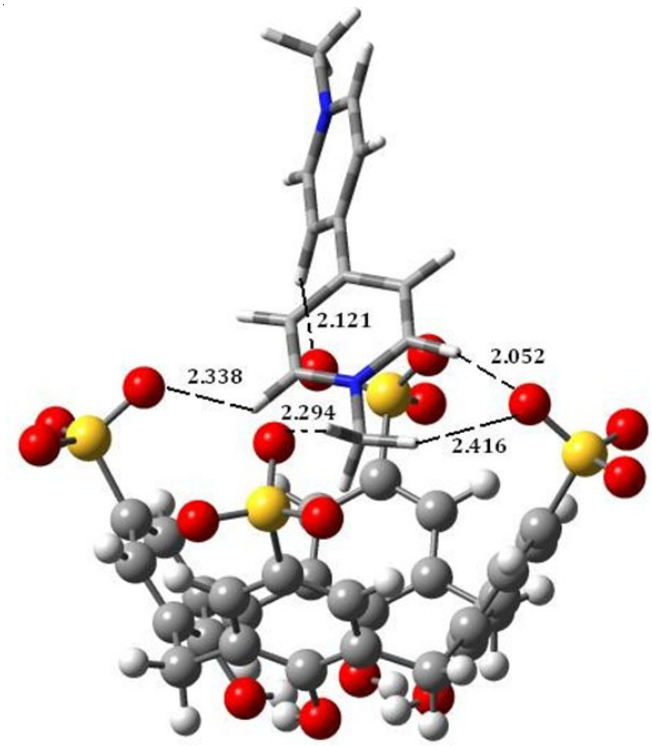

Fig. 4. Lowest energy CX[4]-S-MV^{2+} complex. Interaction energy (kJ mol^{-1}) are given in parentheses

TABLE-2
ELECTRON DENSITY AT BOND CRITICAL POINT IN (ρ_{bcp} IN au) IN CX[4]-S-MV^{2+} COMPLEX

	CX[4]-S-MV^{2+}
C–H···O	2.052 (0.0217)
	2.121 (0.0202)
	2.294 (0.0137)
	2.338 (0.0138)
	2.418 (0.0114)

hydrogen bonded interactions. Selected optimized geometrical parameters of CX[4]-S, MV^{2+} and their complexes from the SCRF-PCM theory are reported in Table-3. As may readily be noticed the oxygens from opposite monomers of CX[4]-S (3.748 Å) exhibited a larger separation on complexation with MV^{2+} (3.782 Å). Likewise, neighboring ring oxygens of CX[4]-S were separated by 0.025 Å in its MV^{2+} complex. The two pyridine rings in MV^{2+} orient mutually at an angle of 141º in isolated guest which on complexation with CX[4]-S was twisted by 10º.

Frontier orbitals HOMO and LUMO are depicted (isosurface of 0.02 a.u.) in Fig. 5. It is clear that the electron-rich regions in the complex as well as the macrocycle receptor CX[4]-S were largely localized near SO_3^- substituents. Moreover, CX[4]-S with MV^{2+} reduces the energy gap of frontier orbitals (HOMO and LUMO) to 1.6 eV compared to 5.2 eV in the isolated guest. The complexation of MV^{2+} with CX[4]-S can be monitored by pursuing the changes in signals of α-, β-, and CH_3 guest protons. The gas phase structures from the present calculations show deshielding of all α-, β-protons of CX[4]-S-MV^{2+} complex in ^1H NMR spectra compared to isolated MV^{2+} guest (Table-4). Bagno *et al.* [42] have concluded that ^1H NMR chemical

TABLE-3
SCRF-PCM OPTIMIZED GEOMETRICAL PARAMETERS (BOND DISTANCES IN Å AND BOND ANGLES IN °) IN CX[4]-S-MV^{2+} AND THEIR RADICAL CATION ANALOGS

	CX[4]-S	MV^{2+}	CX[4]-S-MV^{2+}	$MV^{+\bullet}$	CX[4]-S-$MV^{+\bullet}$
O1–H1	0.991	–	0.990	–	0.991
O1–C1	1.378	–	1.379	–	1.378
C1–C2	1.407	–	1.408	–	1.408
C2–C7'	1.527	–	1.526	–	1.528
C2–C3	1.399	–	1.398	–	1.399
C3–C4	1.394	–	1.395	–	1.394
C4–C5	1.395	–	1.394	–	1.395
C5–C6	1.396	–	1.397	–	1.397
C6–C1	1.525	–	1.525	–	1.526
C6–C7	1.407	–	1.406	–	1.407
C2–C7–C6	113.7	–	112.9	–	114.2
C7–C6–C1	121.3	–	121.3	–	121.3
C6–C1–O1	117.0	–	117.1	–	116.9
O1–C1–C2	121.0	–	121.1	–	121.0
C1–C2–C7'	122.2	–	122.2	–	122.3
C1–C2–C3	117.9	–	118.0	–	117.8
C2–C3–C4	121.2	–	121.1	–	121.2
C3–C4–C5	119.8	–	119.8	–	120.0
C4–C5–C6	120.9	–	120.3	–	120.1
C5–C6–C1	118.2	–	118.4	–	118.2
C1-H1$_\alpha$	–	1.082	1.085	1.082	1.085
C2-H2$_\beta$	–	1.083	1.086	1.082	1.083
C3-C3'	–	1.483	1.483	1.432	1.488
C6-N1	–	1.483	1.482	1.468	1.467
C2-C3-C3'-C4'	–	141.0	132.0	177.5	179.0

shifts (δ_H) in glucose obtained by employing the optimized geometry in solvent modeled *via* SCRF calculations agreed better with the experimental NMR spectra than those derived from gas phase structure. CX[n]-S host possesses three types of protons, (a) hydroxyls from intramolecular interactions (H1), (b) aromatic protons (H3/H5), (c) methylene protons (H7′ and H7″). ^1H NMR chemical shifts in CX[n]-S follow the trend: H1 > H3/H5 > H7′ > H7″ in isolated as well as in their complexes. On complexation with MV^{2+}, H1 and H3 protons of CX[4]-S exhibit up-field signals at δ_H = 9.95 ppm and 7.29 ppm, respectively. The corresponding signals in isolated CX[4]-S were at the δ_H = 10.31 and 7.44 ppm. The δ_H values of H7′ and H7″ were nearly unchanged after complexation. The NMR chemical shifts in MV^{2+} follow the order: $H1_\alpha > H2_\beta > CH_3$, which is in consonant with experimental NMR spectra (in acidic medium). Average δ_H values in MV^{2+} and its CX[4]-S complex are given in Table-5. Moreover, qualitatively different host-guest binding patterns in CX[4]-S-MV^{2+} reflect in δ_H values. Thus hydrogen bonded interactions with host portals led to deshielded signals (δ_H = 10.04 ppm) for H1α proton in the CX[4]-S-MV^{2+} complex. On the other hand, non-interacting H1α protons exhibit up-field signals (δ_H = 8.49 ppm) compared to those for isolated MV^{2+} (δ_H = 8.80 ppm). The experimental Δδ (change in δ_H values on complexation) of MV^{2+} protons for CX[4]-S-MV^{2+} complex follow the order of CH_3 > α-H > β-H. Theoretical ^1H NMR revealed the shielding for protons void of C-H···O interactions with host portals. Thus for non-bonded protons, the changes in δ_H values on complexation match well with those observed in experiment (in acidic medium). Furthermore host-

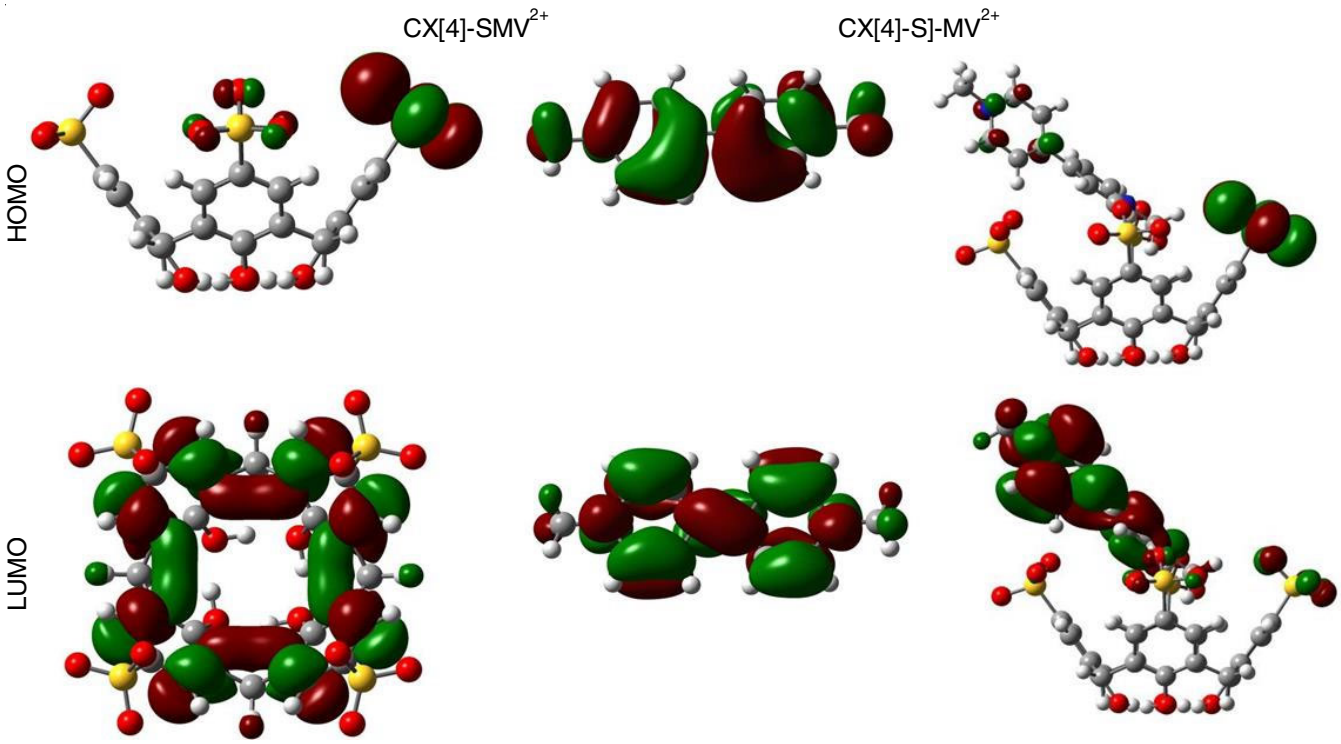

Fig. 5. Frontier orbitals in CX[4]-S-MV^{2+} complexes (iso-surface of ± 0.02 au)

TABLE-4
NMR CHEMICAL SHIFTS (δ_H, IN ppm) OF CX[4]-S COMPLEXES (WITH WATER AS SOLVENT) AT B3LYP/6-31G(d,p), M06/6-31G(d,p) AND B3LYP/6-31G++(d,p) LEVELS

	B3LYP/6-31G(d,p)			M06/6-31G(d,p)			B3LYP/6-31G++(d,p)		
	CX[4]-S	MV^{2+}	CX[4]-S-MV^{2+}	CX[4]-S	MV^{2+}	CX[4]-S-MV^{2+}	CX[4]-S	MV^{2+}	CX[4]-S-MV^{2+}
H1	12.24	–	10.14	10.70	–	9.14	11.13	–	10.72
H3	7.50	–	7.51	7.78	–	7.72	7.82	–	7.62
H5	7.51	–	7.34	7.80	–	7.70	7.81	–	7.38
H7'	4.22	–	3.98	3.75	–	3.90	4.46	–	4.30
H7"	3.49	–	3.32	3.35	–	3.37	3.79	–	3.39
$H1_\alpha$	–	8.86	9.81	–	9.07	9.87	–	8.86	9.52
$H2_\beta$	–	8.35	9.46	–	8.46	9.67	–	8.44	9.26
CH_3	–	4.54	6.80, 4.04	–	4.63	5.67[a], 4.06	–	4.56	7.10[b], 3.89[a]
CH_3'	–	4.54	6.82, 4.03	–	4.63	5.58[a], 3.98	4.56	7.10b	3.89[a]

[a]Average δ_H for protons those are interacting with host portal; [b]Average δ_H for the non-interacting protons

TABLE-5
NMR CHEMICAL SHIFTS (δ_H, IN ppm) OF CX[4]-S COMPLEXES (WITH WATER AS SOLVENT)

	CX[4]-S	MV^{2+}	[Ref. 27]	CX[4]-S-MV2+	[Ref. 27]	[Ref. 27]
H1	10.31	–	–	9.95	–	–
H3	7.44	–	–	7.29	–	–
H5	7.46	–	–	7.49	–	–
H7'	3.98	–	–	3.97	–	–
H7"	3.34	–	–	3.35	–	–
$H1_\alpha$	–	8.80	8.70	10.04[a], 8.49[b]	7.70	7.50
$H2_\beta$	–	8.34	8.30	10.40[a], 7.94[b]	7.50	7.20
CH_3	–	4.47	4.20	2.98	2.80	3.40
CH_3'	–	4.47	–	4.51[a], 4.26[b]	–	–

[a]Average δ_H for protons those are interacting with host portal; [b]Average δ_H for the non-interacting protons

guest complexes between CX[4]-S with methyl viologen radical cation ($MV^{+\bullet}$) are displayed in Fig. 6 and the interaction energies are given in parentheses. It may be remarked here that binding of $MV^{+\bullet}$ to CX[4]-S host were strikingly similar to cationic guest. Calculated interaction energies in case of cationic complex are larger than those in $MV^{+\bullet}$ radical analog. The cyclic voltametry experiments [27] revealed π-e-acceptor and H-bond donor ability of MV^{2+} decreases upon one electron reduction destabilizing CX[n]-S-$MV^{+\bullet}$ complexes. These observations concurred with inferences drawn from the present B3LYP calculations.

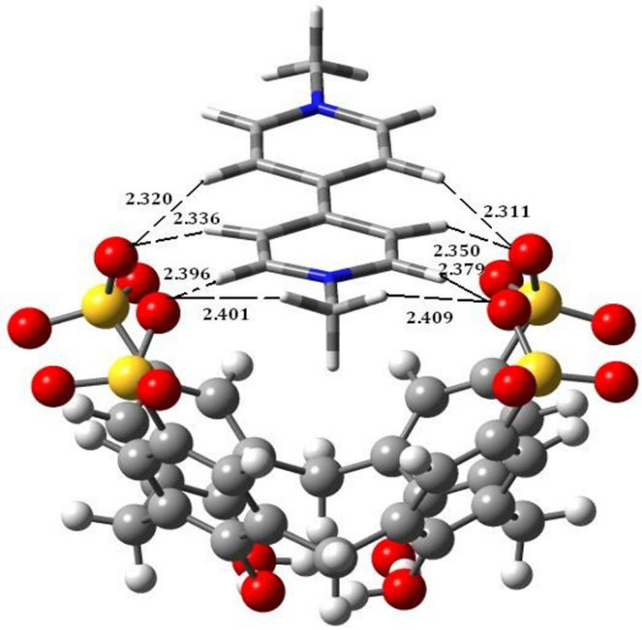

CX[4]-S-MV$^{+\bullet}$ (60.8)

Fig. 6. Lowest energy CX[4]-S-MV$^{+\bullet}$ complexes

Conclusion

Host-guest interactions of MV^{2+} or its radical cation with CX[4]-S hosts were analyzed within the framework of density functional theory. In the lowest energy structures, one of the methyl groups of MV^{2+} was partially penetrating within the cavity of CX[4]-S host owing to C-H···O interactions with upper rim of host while the remaining methyl group excluded from the cavity. Both methyl viologen radical and its dication bind to CX[4]-S in a qualitatively similar fashion. The interaction energies of methyl viologen dication and radical cation in the host-guest complexes suggested that dication binds strongly than its radical cation to CX[*n*]-S hosts.

CONFLICT OF INTEREST

The authors declare that there is no conflict of interests regarding the publication of this article.

REFERENCES

1. C.D. Gutsche, Monographs in Supramolecular Chemistry: Calixarenes; The Royal Society of Chemistry: Cambridge, U.K., vol. 1. (1989).
2. C.D. Gutsche and I. Alam, *Tetrahedron*, **44**, 4689 (1988); https://doi.org/10.1016/S0040-4020(01)86171-8
3. C.D. Gutsche, ed.: E. Weber, Host Guest Complex Chemistry Macrocycles: Synthesis, Structures and Applications, Springer: Berlin (1985).
4. C.D. Gutsche, Calixarenes Revisited, Monographs in Supramolecular Chemistry, The Royal Society of Chemistry: Cambridge, UK (1998).
5. N. Douteau-Guével, A.W. Coleman, J.P. Morel and N. Morel-Desrosiers, *J. Phys. Org. Chem.*, **11**, 693 (1998); https://doi.org/10.1002/(SICI)1099-1395(1998100)11:10<693::AID-POC18>3.0.CO;2-8
6. O.I. Kalchenko, F. Perret, N. Morel-Desrosiers and A.W.A. Coleman, *J. Chem. Soc. Perkin. Trans. II*, 258 (2001); https://doi.org/10.1039/b005497f
7. A. Dondoni and A. Marra, *Chem. Rev.*, **110**, 4949 (2010); https://doi.org/10.1021/cr100027b
8. J. Vicens and V. Bohmer, Calixarenes: A Versatile Class of Macrocyclic Compounds. Kluwer Academic Publishers: Dordrecht, Boston (1991).
9. S. Ikeda and S. Shinkai, *Chem. Rev.*, **97**, 1713 (1997); https://doi.org/10.1021/cr960385x
10. V. Böhmer, *Angew. Chem. Int. Ed. Engl.*, **34**, 713 (1995); https://doi.org/10.1002/anie.199507131
11. A. Suwattanamala, A.L. Magalhães and J.A.N.F. Gomes, *J. Mol. Struct. THEOCHEM*, **729**, 83 (2005); https://doi.org/10.1016/j.theochem.2005.03.060
12. N. Iki, F. Narumi, T. Fujimoto, N. Morohashi and S. Miyano, *J. Chem. Soc. Perkin Trans. II*, 2745 (1998); https://doi.org/10.1039/a803734e
13. S. Seiji, A. Koji, T. Takayuki, A. Takashi and M. Osamu, *J. Chem. Soc. Perkin Trans. II*, 2297 (1987).
14. H. Bakirci, A.L. Koner and W.M. Nau, *J. Org. Chem.*, **70**, 9960 (2005); https://doi.org/10.1021/jo051689z
15. S. Shinkai, K. Araki, T. Matsuda, N. Nishiyama, H. Ikeda, I. Takasu and M. Iwamoto, *J. Am. Chem. Soc.*, **112**, 9053 (1990); https://doi.org/10.1021/ja00181a004
16. G. Arena, A. Casnati, A. Contino, F.G. Gulino, D. Sciotto and R. Ungaro, *J. Chem. Soc., Perkin Trans. II*, 419 (2000); https://doi.org/10.1039/a909847j
17. K. Wang, D.S. Guo, H.Q. Zhang, D. Li, X.L. Zheng and Y. Liu, *J. Med. Chem.*, **52**, 6402 (2009); https://doi.org/10.1021/jm900811z
18. H. Weidel and M. Russo, *Monatsh. Chem.*, **3**, 850 (1882); https://doi.org/10.1007/BF01516855
19. E.L. Clennan, *Coord. Chem. Rev.*, **248**, 477 (2004); https://doi.org/10.1016/j.ccr.2004.01.001
20. C.L. Bird and A.T. Kuhn, *Chem. Soc. Rev.*, **10**, 49 (1981); https://doi.org/10.1039/cs9811000049
21. L.A. Summers, The Bipyridinium Herbicides, Academic Press: New York (1980).
22. D. Meisel, W.A. Mulac and M.S. Matheson, *J. Phys. Chem.*, **85**, 179 (1981); https://doi.org/10.1021/j150602a015
23. P.M.S. Monk, The Viologens. Physicochemical Properties, Synthesis and Applications of the Salts of 4,4′-Bipyridine, John Wiley & Sons: Chichester, U.K. (1998).
24. J.M. Lu, S.V. Rosokha and J.K. Kochi, *J. Am. Chem. Soc.*, **125**, 12161 (2003); https://doi.org/10.1021/ja0364928
25. W. Ong and A.E. Kaifer, *J. Org. Chem.*, **69**, 1383 (2004); https://doi.org/10.1021/jo035030+
26. K. Wang, S.-Y. Xing, X.-G. Wang and H.-X. Dou, *Org. Biomol. Chem.*, **13**, 5432 (2015); https://doi.org/10.1039/C5OB00053J
27. D.S. Guo, L.H. Wang and Y. Liu, *J. Org. Chem.*, **72**, 7775 (2007); https://doi.org/10.1021/jo701304g
28. P. Politzer, Chemical Applications of Atomic and Molecular Electrostatic Potentials, Plenum: NewYork (1981).
29. G. Naray-Szabo and G.G. Ferenczy, *Chem. Rev.*, **95**, 829 (1995); https://doi.org/10.1021/cr00036a002
30. S.R. Gadre, S.A. Kulkarni and I.H. Shrivastava, *J. Chem. Phys.*, **96**, 5253 (1992); https://doi.org/10.1063/1.462710
31. S.R. Gadre and R.N. Shirsat, Electrostatics of Atoms and Molecules. Universities Press: Hyderabad, India (2000).
32. A.D. Becke, *J. Chem. Phys.*, **98**, 5648 (1993); https://doi.org/10.1063/1.464913
33. C. Lee, W. Yang and R.G. Parr, *Phys. Rev. B Condens. Matter*, **37**, 785 (1988); https://doi.org/10.1103/PhysRevB.37.785
34. Y. Zhao and D.G. Truhlar, *Theor. Chem. Acc.*, **120**, 215 (2008); https://doi.org/10.1007/s00214-007-0310-x
35. M.J. Frisch *et al.*, Gaussian 09, Gaussian Inc.: Wallingford (2009).
36. P. Balanarayan and S.R. Gadre, *J. Chem. Phys.*, **119**, 5037 (2003); https://doi.org/10.1063/1.1597652
37. A.C. Limaye and S.R. Gadre, *Curr. Sci.*, **80**, 1296 (2001).
38. R.F.W. Bader, Atoms in Molecules: A Quantum Theory, Oxford University Press: Oxford, U.K. (1990).
39. D.F. Matta and R.J. Boyd, The Quantum Theory of Atoms in Molecules, An Introduction to the Quantum Theory of Atoms in Molecules, Wiley-VCH: Weinheim, pp. 1-34 (2007).
40. K. Wolinski, J.F. Hinton and P. Pulay, *J. Am. Chem. Soc.*, **112**, 8251 (1990); https://doi.org/10.1021/ja00179a005
41. S. Miertuš, E. Scrocco and J. Tomasi, *Chem. Phys.*, **55**, 117 (1981); https://doi.org/10.1016/0301-0104(81)85090-2
42. A. Bagno, F. Rastrelli and G. Saielli, *J. Org. Chem.*, **72**, 7373 (2007); https://doi.org/10.1021/jo071129v